ARTICLE

Optimizing the Structure and Yield of Vanadium Oxide Nanotubes by Periodic 2D Layer Scrolling

Received 00th January 20xx,
Accepted 00th January 20xx

DOI: 10.1039/x0xx00000x

www.rsc.org/

David McNulty[a,b], D. Noel Buckley[a] and Colm O'Dwyer*[b,c]

Metal oxide nanotubes with wide interlayer van der Waals spaces are important materials for a range of applications from energy storage to catalysis, and from energy efficient metal-insulator systems to smart window technologies. Controlling the crystalline quality is critical for the material's physical properties on the nanoscale. We report a systematic investigation into the optimization of structural quality and yield of vanadium oxide nanotubes (VONTs) synthesized by hydrothermal treatment. Usually, interdigitation of alkyl-amine chains occurs between V_2O_5 lamina, a stitching process that allows scrolling of 2D crystalline sheets into nanotubes with consistently high quality. Through detailed microscopy and spectroscopy examination, we demonstrate that two amine molecules per V_2O_5 unit optimizes the structure, quality and yield of the VONTs, and that uniform coverage of the juxtaposed V_2O_5 surfaces in the interlayer spacing minimizes non-uniformities and defects. This observation is consistent for a range of primary amine lengths (hexylamine to hexadecylamine). Through statistical investigation of hundreds of VONTs under each condition, we uncover the effect of amine chain length of V_2O_5 2D sheet thickness, and mechanism for optimum VONT quality. Finally, we summarize non-uniformities during VONT synthesis including, bending, spiraling and twisting of the scrolled crystalline layers.

Introduction

Low-dimensional nanomaterials such as nanotubes [1-3] and nanowires [4-6] have been investigated in detail because of their novel and often functional properties, which has led to their research and development for potential applications in energy storage [7], electronics [8], sensing [9] and catalysis [10]. Most nanomaterials offer unusual (different from bulk) properties endowed by confined dimensions, and the overall behaviour can often exhibit a combination of bulk and surface properties [11, 12]. Metal-oxide nanostructures have been prepared by a variety of processes, from bottom-up direct synthetic protocols to top-down electrochemical etching of oxidized metals [13-15]. A range of metal oxide nanostructures have been reported including nanorods, nanowires, nanobelts and fiber-shaped materials [16-19].

Vanadium oxides and their derivative compounds have attracted a great deal attention because of their outstanding physical and chemical properties and their versatility in terms of potential applications in various areas including as catalysts, sensors and battery electrode materials. [20, 21] Various low-dimensional vanadium oxide-based materials have been studied extensively [22-25]. Starting from the laminar V_2O_5 xerogel [26] numerous two and three dimensional organic-inorganic intercalation products have been obtained [27-30]. Hybrid or templated V_2O_5 nanomaterials have demonstrated useful functions, particularly in energy storage [31, 32]. For example, alkyl-vanadium oxide hybrids have been demonstrated to influence charge capacities and accommodate structural changes in layered battery materials when charged and discharged [33], and layered V_2O_5 has recently being examined as a positive electrode material for Na-ion batteries. [34, 35] Vanadium oxide nanotubes (VONTs) are a primary example of a 'classic' nanotube exhibiting a hollow core flanked by periodic layers of material reminiscent of multi-walled carbon nanotubes [36, 37]. In reality, VONTs are actually nanoscrolls, where once single lamina folds around itself to form either a helical or non-helical tubular structure with a hollow core whose diameter is defined by the radius of curvature of the initial innermost scroll. To realize these structures, the introduction of organic templates is often needed. Some exceptions do exist, namely the class of misfit layered compounds that scroll into chiral tubes formed by relatively planar orientations with different stacking orders of the crystalline layers. [38] Soft chemistry routes have been reported for many organic-inorganic interactions involving layered materials, where the organic phase intercalates into the van der Waals spaces in layered materials such as oxides [39, 40], layered double hydroxides [41, 42], and transition metal dichalcogenides [43, 44].

A key element in the rational design of hybrid organic-inorganic nanostructures is control of surfactant packing and

[a] *Department of Physics and Energy, Charles Parsons Initiative on Energy and Sustainable Environment, and Materials & Surface Science Institute University of Limerick, Limerick, V94 T9PX, Ireland*
[b] *Department of Chemistry, University College Cork, Cork, T12 YN60, Ireland*
[c] *Micro-Nano Systems Centre, Tyndall National Institute, Lee Maltings, Cork, T12 R5CP, Ireland*
† Email: c.odwyer@ucc.ie
Electronic Supplementary Information (ESI) available: [Additional interlayer spacing measurements and FTIR data]. See DOI: 10.1039/x0xx00000x

adsorption onto the inorganic phase in crystal growth and assembly. A significant effort has been made to control morphologies of transition-metal oxides including vanadium oxide nanostructures. A wide variety of organic species from simple primary amines to more complex organic moieties have been used to organize vanadium oxides into complicated three-dimensional structures [45-48]. A common feature is the formation of alternating layers, with the organic phase sandwiched between a crystalline bilayer of vanadium oxide; this can be found in both layers and scrolled lamina within VONTs.

Experimental techniques such as high resolution microscopy and spectroscopy provide a wealth of information on the structure and properties of layered nanostructured materials, and may be complemented by nanoscale models that provide atom-scale structure, dynamics and energetics. The detailed structural analysis, however, is critical for examination of synthetic protocols, particularly since batch to batch variation is well known in the community. For vanadium oxides, many reported nanostructures stem from unforeseen changes in synthetic parameters, leading to difficulty in exact quality control and reproduction of complex structures and assemblies of these materials. For applications and commercial usage, VONTs produced in large quantities should have consistency in quality and self-similarity. In an effort to improve the consistency of VONTs many different synthesis routes have been investigated [49-53]. At the core of this debate, is the influence and function of the intercalation alkylammonium bilayer that forms between the sheets of the V_2O_5. This interaction is very similar to processes reported for layered organoclays [54, 55], and for intercalation of amphiphilic phases in classic 2D crystals comprising layered smectic materials such as montmorillonites [56]. The factors that determine the uniformity and optimum shape of high quality VONTs have not been formally investigated despite the many variations of VONTs using different organic templates [57].

Through high resolution microscopy, vibrational spectroscopy and diffraction based analyses, we report the first systematic investigation into synthetic factors that affect VONT characteristics and we define the best synthetic conditions for high yield of optimized VONTs. Herein, we detail VONTs prepared with amines that have both shorter and longer molecular lengths than the most traditionally used amines. Through TEM measurements and XRD analysis we quantify the effect of intercalating amine molecules of different lengths between layers of vanadium oxide bound by van der Waals interactions – we examine alkyl amines from hexylamine to didecylamine. By varying the molar ratio of vanadium oxide precursor to amine surfactant, we probe the VONT growth mechanism and determine the effects of excess of either vanadium oxide precursor or amines prior to hydrothermal treatment on the resulting uniformity and yield. In the case of a limiting quantity of amine structural templates, we show for the first time that a low yield of good quality VONTs forms at the expense of lower yield, confirming a preferential interdigitation rather than reaction process. Additionally, the data shows how the interdigitated amines not only maintain the resulting VONT structure, but help define its structure and importantly, the yield of self-similar VONTs. The effect of amine length on vanadium oxide sheet thickness that scroll within the VONTs structures is determined by statistical analysis of HRTEM images. We also detail the non-uniformities that are present in small quantities of VONTs after the synthesis process.

Results and discussion

During hydrothermal treatment the amine templated vanadium oxide layers undergo scrolling to form the eventual nanotube [52, 58, 59], as shown schematically in Fig. 1(a). There are three main stages that have been assigned to VONT formation: (i) the initial lamellar crystalline xerogel, (ii) an intermediate stage where scrolling is initiated and intercalation of the template has occurred, and (iii) the final stage where the intercalated layers accommodate the uniaxial scrolling to form the VONT. The initial stage occurs during the two days of mixing and aging prior to the hydrothermal treatment. It is during this time that the amine molecules are intercalated between the layers of vanadium oxide xerogel, as a bilayer stacked back-to-back between the (010) faces of the V_2O_5 sheets [60]. The hollow core and tube openings are clearly seen in the SEM image of a bundle of VONTs in Fig. 1(b). The scrolled nature of the VONTs can be seen in the cross section of the tube openings, shown in Fig. 1(b). The length of VONTs can vary from a few hundred nanometers to micrometers, as shown in the low magnification TEM image in Fig. 1(c), and only very recently has controlled over the length of VONTs been reported. [61]

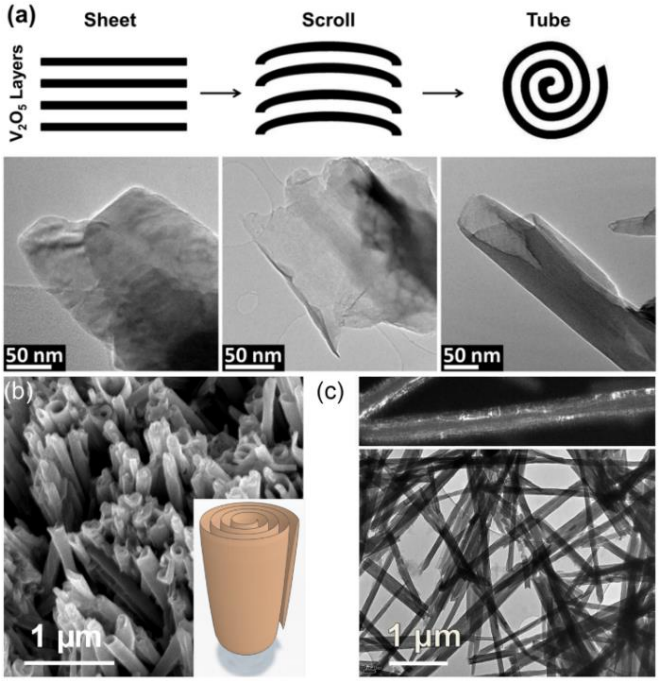

Fig. 1. (a) Schematic of the growth mechanism of a scrolled nanotube with corresponding TEM images from early (individual amine-functionalized lamella), intermediate (initiation of scrolling) and final stages of VONT formation. (b) SEM image showing a bundle of VONTs (c) Low magnification TEM image of VONTs. Inset is a dark field STEM image of a single VONT confirming the scrolls of crystalline V_2O_5 material around the hollow core.

Even though VONTs are essentially scrolled layers of vanadium oxide, HRTEM data gives an accurate value for this spacing at high magnification where the degree of curvature negligibly affects the true measurement of interlayer and periodic spacing. Quantifying the spatial correlations from a comparison of XRD data to TEM images from a corresponding sample allows parallel examination of periodic values from a large volume of VONTs in XRD data with defined measurement of representative VONTs from each sample using TEM, thereby minimizing the limitations of either technique on its own. HRTEM is used to assess the true nanosheet lamina thickness separate from its periodicity, and the degree of crystallinity deconvoluted from X-ray reflections of higher intensity from layered periodicity.

The amine template occupies the interlayer spacing and there are several possible configurations in which this can occur, which are illustrated schematically in Fig. 2. Figure 2(a) shows amine molecules aligned collinearly tail to tail and perpendicular to the V_2O_5 layers, Fig. 2(b) shows amine molecules aligned collinearly tail to tail at an angle α to the V_2O_5 layers, Fig. 2(c) shows interdigitated amine molecules at an angle α to the V_2O_5 layers and Fig. 2(d) shows amine molecules interdigitated and perpendicular to the V_2O_5 layers. In Fig. 2(a) the interlayer spacing is approximately twice the length of the amine molecule, *i.e.* ~ $2l_{mol,}$ while in Fig. 2(b), (c) and (d) it is less than $2l_{mol}$. From molecular-dynamics simulations [62] of alkanethiol packing in the V_2O_5 interlayer spacings, the tilted bilayer formation without interdigitation is energetically less favorable, particularly for longer chains; the upright alkyl chains packed on the basal surface without a greater degree of chain overlap is a feasible energy minimized structure for the consistent spacing in the scrolling of the VONTs during growth. Alkylamines with n = 6 or less C-C bonds typically lie flat on the V_2O_5 surface.

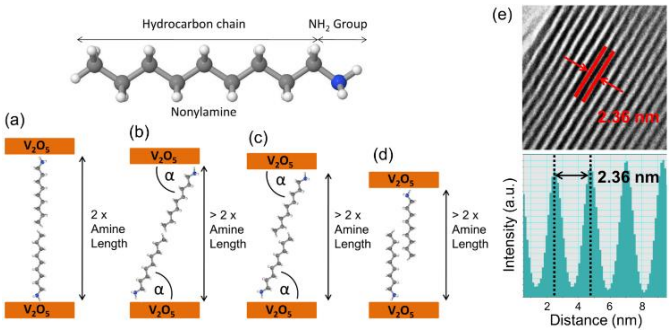

Fig. 2. Schematic of the bilayer of amine chains intercalated between layers of V_2O_5 (a) amine chains standing tail on tail, perpendicular to the layers of V_2O_5 (b) amine chains standing tail on tail, at an angle α to the layers of V_2O_5 (c) amine chains interdigitated parallel to each other at an angle α to the layers of V_2O_5 (d) amine chains interdigitated parallel to each other and perpendicular to the layers of V_2O_5. (e) TEM image and greyscale map of interlayer spacing measurement by TEM. Vanadium is a heavier electron scatterer and appears as periodic dark parallel features and in this manner the interlayer spacings can be measured.

Quantifying synthetic parameters that modify VONT quality and uniformity

To distinguish between these configurations and to examine the effect of amine molecular length, we experimentally determined the interlayer spacings by statistical analysis of a multitude of TEM images and XRD patterns of VONTs synthesized with different V_2O_5:amine ratios and different amine lengths (*vide infra*). An example of an interlayer spacing measurement taken from a TEM image is shown in Fig. 2(e). The degree of interdigitation was also estimated geometrically as discussed in the Supplementary Information (Fig. S1).

The synthesis of VONTs with dodecylamine and hexadecylamine has previously been reported in the literature [36, 63, 64], and has been a standard synthetic protocol. However, in the systematic study presented in this work, a range of primary amines ranging in structure length from n = 6 – 20 C-C bonds were used, in addition to a controlled variation in the xerogel:amine molar ratio. We chose this range to determine if VONTs can form using very short amine molecular templates, and to investigate the influence of the template packing density (number of amines per unit V_2O_5) and order on the resulting quality of the scrolled VONT.

Figures 3(a)-(g) show typical TEM images of VONTs synthesized using a molar ratio of xerogel:amine of 1:2, for a range of amine templates with different nominal lengths. In all cases, the characteristic nanotube morphology is found, and each synthesis produced a product consisting of VONTs with small amounts of unreacted V_2O_5. It was found that V_2O_5 xerogel mixtures with primary amines ranging from n = 6 to 18 C-C bonds undergo a topotactic reaction whereby the cohesive structure of the layered vanadium oxide xerogel is maintained and the definitive VONT structure is mediated by intercalation and binding of an ordered bilayer of interdigitated amine molecules. A consistent scroll into a VONT is also observed even in cases where the xerogel:amine ratio has been reversed (limited amine quantity).

All syntheses with didecylamine, the non-primary amine used in this study, proved unfruitful and exfoliated crystalline nanobelts rather than VONTs were formed, as shown in Fig. 3(h). Experimental syntheses using vanadium triisopropoxide as a precursor also successfully formed VONTs for the shorter amines investigated here, but consistently, the use of didecylamine in all mixture ratios, with the isopropoxide precursor and also with the V_2O_5 sol-gel did not form VONTs. While flat-lying amines are expected when the chain length n < 6, it has been proposed that more upright standing interdigitated amines are found for longer chain lengths, typically n > 12. We previously determined that the upright ordering and packing of longer amines is stable only when interdigitation occurs, which prevents disassembly and delamination during the development of curvature in the VONT scrolling step. However, for didecylamine, its structure comprises a decyl chain either side of the amine group, preventing electrostatic binding of the amino group to the V_2O_5 basal surface under the reducing conditions where scrolling occurs with all primary alkylamines. Thus, effective

adsorption and formation of the interdigitated bilayer that is a pre-requisite to scrolling of layers into the VONT structure, requires a free, charged deprotonated amino head-group. Syntheses with didecylamine provides a direct test of the binding mechanism. Previous syntheses that have used alternatives to primary alkylamines have involved diamines and other molecular templates for example [36], allowing two head-groups for binding. Didecylamine (and dipentylamine and similar species) are thus shown here to be completely ineffective in promoting and maintaining layer scrolling to form VONTs.

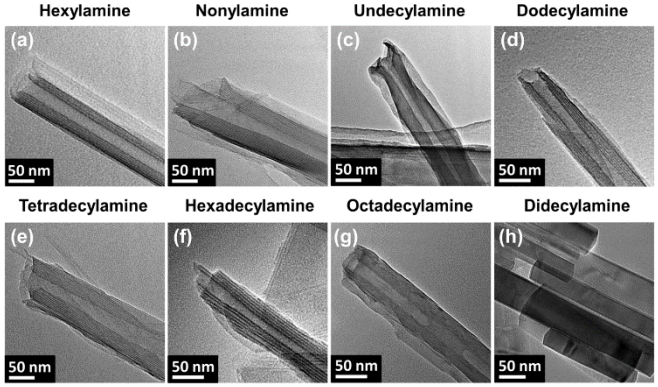

Fig. 3. TEM images of individual nanotubes for VONTs synthesized with a V_2O_5:amine ratio of 1:2 using (a) hexylamine, (b) nonylamine, (c) undecylamine, (d) dodecylamine, (e) tetradecylamine, (f) hexadecylamine and (g) octadecylamine. (h) TEM image of flat nanobelts formed as a result of hydrothermal treatment of V_2O_5 xerogel and didecylamine.

During the initial aging stage during HT, the amines are hydrolyzed by water to form alkyl ammonium ions and hydroxide ions. The reaction is as follows:

$$C_nH_{(2n+1)}NH_2 + H_2O \rightarrow C_nH_{(2n+1)}NH_3^+ + OH^- \qquad \text{(Eqn 1)}$$

The resulting hydroxide ions break down the V=O bond present in the V_2O_5 molecule to form (V–OH) and ($V–O^-$) bonds, in this manner the vanadium becomes six-coordinated while developing an effectively dual V^{4+}/V^{5+} oxidation state. The attachment of the amine is generally accepted to be an electrostatic bond between the oxidized amino head group (NH_3^+) and the reduced vanadyl ($V–O^-$) bond with complex entropy maximized van der Waal's interactions between the hydrocarbon chains of the intercalated amines. [59] However, the results show that to form a VONT of any quality, the charged state of the free amino headgroup is necessary. This stitching of hydrocarbon chains maintains the characteristic and consistent layered structure of vanadium oxide during scrolling.

For VONTS, the real reason for curvature without cleavage or delamination is not entirely clear, but is likely to be a cooperative effect mediated by the ability of the crystal structure to accommodate bending [65], and the organic template to maintain a constant interlayer distance. Tetrahedral $V–O_4$ and square pyramidal $V–O_5$ crystal subunits replicate the structure within VONTs, but such crystallographic analysis omits the influence of the organic intercalant on the net charge and crystalline unit cell structure; stacked V_2O_5 layers comprising $V–O_5$ octahedra described the initial non-curved layer structure very well. We previously determined using molecular dynamic simulations that the organic 'velcro' is an energetic requirement for the maintenance of the curvature in the scrolled structure [66].

Figure 3 shows that when synthesized with an amine packing density that maximizes the available attachment sites on the V_2O_5, a stable and strong amine bilayer can maintain the ordered scrolling. For the inorganic phase, the VO_x substrate formed in the initial stages, outlined in Fig. 1(a), is comprised of the more flexible corner-shared orthorhombic layered subunits, instead of the edge shared monoclinic structure where both $V–O_4$ and $V–O_6$ units of the crystal structure rather than $V–O_5$ units known for the xerogel, accommodate the need for bending during hydrothermal treatment. The high temperature effectively lowers the barrier to bending of the substrate allowing it to occur and form the scrolled nanotubular structure. The degree of allowed bending upon its initiation is likely to define the inner hollow core (radius of curvature of the initial, inner core). Once the first scroll is formed, this possibly dictates the inner hollow core during continuous scrolling, since compressive tightening would likely cause a chiral protrusion of the inner layers, or a collapse of the inner scrolls, which would need to overcome the organic template adhesive between each successive inorganic sheet.

To quantify the layer spacing, crystal structure, overall quality and yield of the VONTs made in Fig. 3 and for a wider range of mixture ratios, experimental syntheses were conducted using short, medium and long length amines in mixture ratios (V_2O_5:amine) of 4:1, 3:1, 2:1, 1:1, 1:2, 1:3, and 1:4. Figure 4 shows TEM images for various scrolled VONTs synthesised using hexylamine, dodecylamine and octadecylamine for a series of different molar ratios of xerogel to amine. From TEM analysis (of VONTs from 21 different syntheses) we found that the synthesised VONTs have outer diameters varying from ~75 to 200 nm. VONTs are formed in all cases; in some cases unreacted V_2O_5 xerogel remains. This is most prevalent in the samples when xerogel is in excess. In some cases, when amines are present in excess, a layer of amines can be seen along the outer surface of the VONT. From TEM analysis it was found that the optimum ratio for producing high quality VONTs is a molar ratio of xerogel to amine of 1:2, i.e. 2 amines per V_2O_5 unit. This molar ratio resulted in the greatest yield of high quality VONTs and a reduction in the amount of unreacted xerogel still present after HT.

The molecule surface attachment sites on the V_2O_5 surface in each stacked layer within the VONT involves the ionised amine molecule binding electrostatically to the reduced vanadyl bonds. In common with alkanethiol adsorption onto V_2O_5 (010) it was previously reported [66] that alternative amine-V_2O_5 binding sites are also possible, in particular due to competition between the surface Brønsted base V-O and in-

plane Lewis base V–O–V oxygens for the amino head groups. Other amine binding sites may also be possible due to oxygen vacancies, surface V^{5+}/V^{4+} ratios, and new surface states formed following, for example, condensation reactions [67]. Such defects can also form at high temperatures >400 °C – such conditions would need to be reached within the high-pressure autoclave at a nominal oven temperature of 180 °C. It was reported from molecular dynamics simulations that alkanethiol molecules which were intercalated within layers of V_2O_5 self-assemble preferentially in a vertically interdigitated, bilayered arrangement between the layers [62].

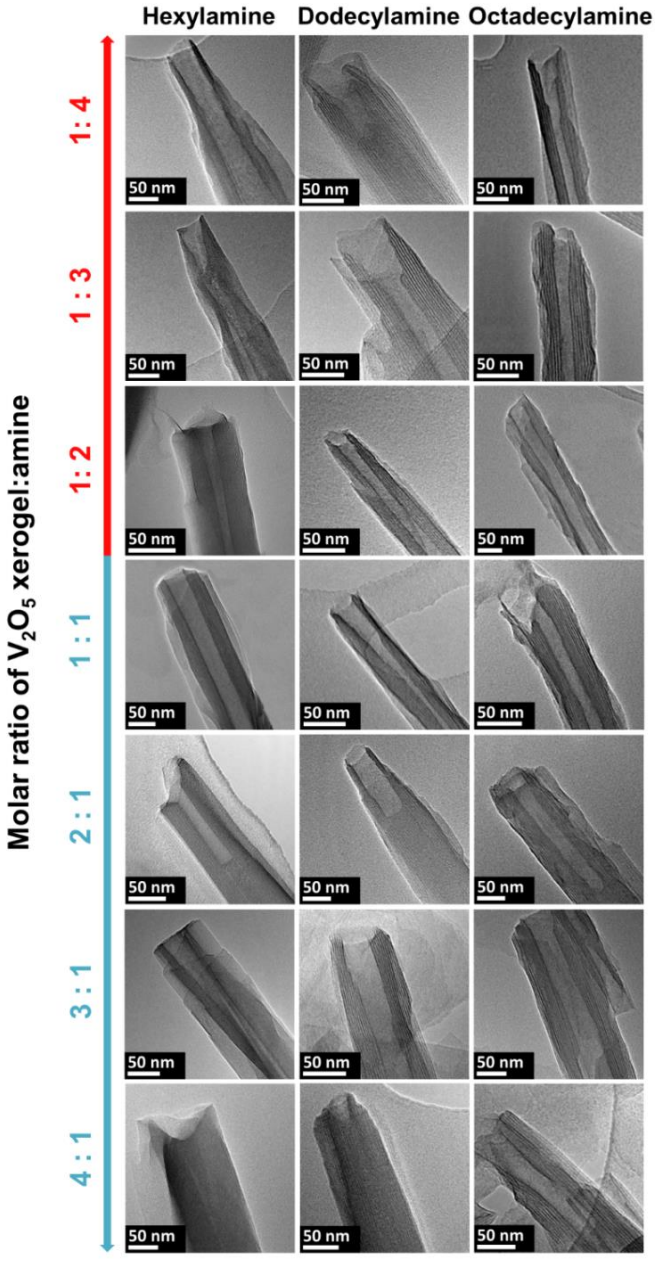

Fig. 4. TEM images of individual VONTs synthesized with various V_2O_5:amine ratios, marked on the left axis, using hexylamine, dodecylamine, and octadecylamine.

XRD patterns obtained from low-angle (3-15°) and high-angle (15-70°) scans for VONTs synthesized using hexylamine, dodecylamine and octadecylamine are shown in Fig. 5, at each of the xerogel:amine ratios from 1:4 to 4:1. XRD patterns from milligram quantities of powder directly probes the periodicity in VONT scrolls and also the crystallinity of the V_2O_5 lamina in large quantities of product. The XRD patterns of VONTs typically show two characteristic regions. The first, low angle region shows the (00*l*) Bragg reflection peaks known to be characteristic of a well-ordered, periodic layered structure consisting of vanadium oxide sheets propped open by an intercalated bilayer of interdigitated amines, stacked periodically back-to-back, in a scrolled fashion. The second region comprises (*hk*0) reflections, indexed to the orthorhombic unit cell from the crystal structure of the V_2O_5. The characteristic (*hk*0) reflections indicate high structural order, and well-formed, scrolled tubes which typically exhibit characteristic asymmetric line-shapes for (*hk*0) reflections (e.g. Fig. 5(b)) from the crystal lattice in a curved layer; defective tubes and unreacted material exhibit reduced intensity reflections or absent reflections from significant deformation of the crystalline V_2O_5 lamella. The periodic (00*l*) reflections for each VONT in Fig. 5(a), (c) and (e) were shifted consistently to lower angles (wider spacing) when successively longer amines are used in synthesis. For VONTs synthesized with octadecylamine (Fig. 5(e)), the resulting periodic spacing is widest, with the corresponding (001) reflections at small angles ($2\theta < 3^o$). We note that the bilayered structure with an absent (002) reflection often observed with non-scrolled laminar vanadates intercalated with thiols or with some layered vanadium oxides intercalated with organic species [68], are not found here for all lengths of primary amine used.

Examination of the crystal structure of the layers also confirms the salient features of the effect of amine length and the molar ratio of xerogel to amine. Figures 5 (b), (d) and (f) show the (*hk*0) reflections for each VONT synthesis, which for all cases occurred at similar diffraction angles, confirming that the V_2O_5 maintains its orthorhombic crystal structure. For the molar ratio at which a lot of unreacted material remains (xerogel:amine = 4:1), the diffraction contribution from the crystal structure of bulk V_2O_5 is ill-defined and some reflections arise from a mixture of monoclinic xerogel and orthorhombic V_2O_5, which forms during hydrothermal treatment. By comparison, the ordered reflections from a xerogel:amine ratio of 1:2 in Fig. 5 for all cases (where the yield of VONTs is much greater), show the characteristic diffraction peaks typical of scrolled, high quality VONTs. In addition, the phase is pure and can be indexed to orthorhombic V_2O_5 with reconstructed lattice parameters of a_0 = 1.152 nm, b_0 = 0.356 nm, c_0 = 0.437 nm; Space Group = P*mnm*, with no peaks of measureable intensity found from other crystalline vanadium oxide phases.

For VONTs prepared using excess amines xerogel:amine of 1:3 and 1:4, respectively) the majority of the characteristic orthorhombic V_2O_5 peaks were not observed. This indicates that for these molar ratios a considerable portion of the xerogel:amine mixture remains unreacted after hydrothermal

treatment. In this work, synthesis parameters such as temperature, pH, duration hydrothermal treatment (HT) time are kept consistent within the autoclave for each synthesis, leaving the relative quality and consistency in VONT production a function of the organic intercalant. Jaber *et al.* [60] also showed from TEM, XANES, and EPR investigations, that once a polyoxovanadate species is formed at the early stages of HT, many forms of V_2O_5 precursor can be used to eventually form VONTs. Here, the precursor (xerogel) is also constant, but we note that it too is a layered, solid structure. Jaber *et al*. also demonstrated via flame spectroscopy that amines are detected within the supernatant after 100 h of HT, indicating a (re)dissolution-precipitation mechanism that results in crystallized regions of V_2O_5. In our case, as all parameters are kept constant for VONT formation aside from amine length, such a mechanism would be exacerbated in the case of an excess xerogel content.

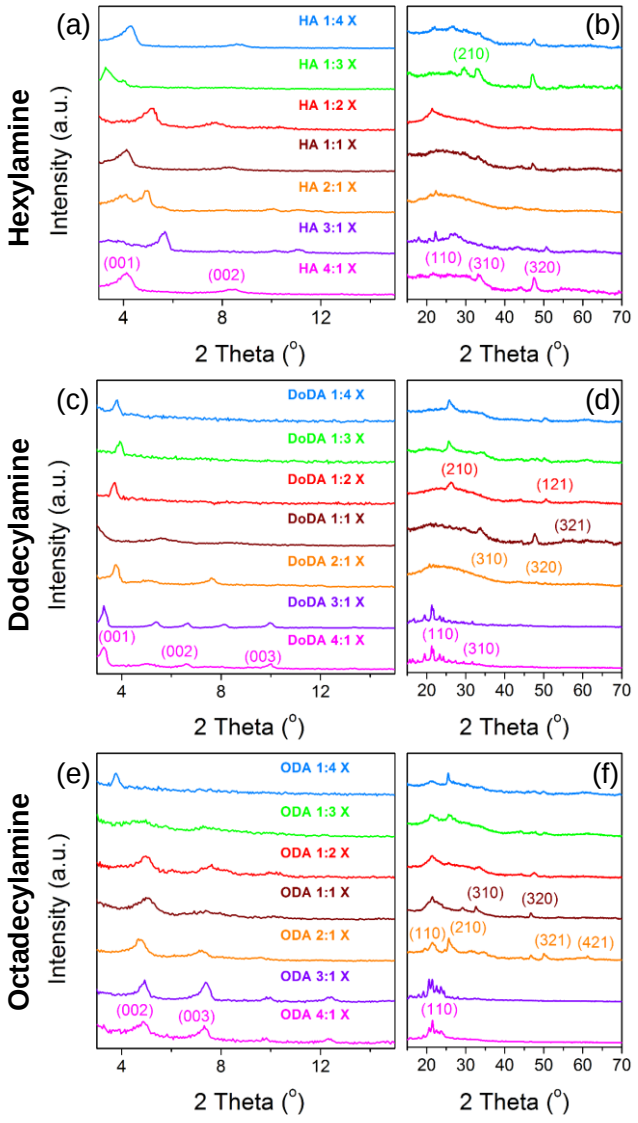

Fig. 5. XRD patterns showing (00*l*) reflections and (*hk*0) reflections from VONTs synthesised using (a) and (b) hexylamine, (c) and (d) dodecylamine, (e) and (f) octadecylamine.

While VONT formation is preferred for limited amine content (as evidenced by TEM of high quality VONTs in small amounts), XRD confirms significant V_2O_5 that is not a layered structure, which may have a contribution from solubilization/removal of intercalated amines over longer durations (> 4 days) from the low quantity of VONTs formed with limited amine content (xerogel:amine ratios > 2:1). With amines in excess however, solubilization is reached more easily without removal of amines that results in large scale collapse of the VONT structure in xerogel:amine ratios < 1:2.

We note that many syntheses of hybrid layered organic-inorganic materials display aperiodicities and shoulder peaks close to the main periodic reflections. In some instances, these have been interpreted as tactoids, which are submicron grains or aggregated stacks close to the edges of interlayer spacings, thus contributing to the primary reflection with a reduced shoulder intensity from a slightly reduced interlayer spacing. Our analysis proves that such features are observed in two cases. The first agrees with other observations, where extra small peaks close to periodic reflections arise from non-uniformities and irregularities in the structure (e.g. local reduction or removal of interlayer spacing as detailed further on). Second, our analyses show that aperiodic reflection can also occur when uniform VONTs or layering is formed in a minority of the product, i.e. some of the material successfully converted topotactically to high quality VONTs with the remainder forming an irregular layered structure that also contributed to the overall XRD pattern. This second observation is confirmed via microscopy and vibrational spectroscopic investigations outlined in the next sections.

Periodic spacing in scrolled VONTs: Lamina thickness, interlayer spacing and the role of amines on the VONT structural quality

In order to accurately measure the V_2O_5 lamina thickness, interlayer spacing occupied by the amine bilayers and the overall periodic spacing in large quantities of VONTs from all syntheses, the periodic spacing values determined from XRD analysis are summarised in Fig. 6(a), and Fig. S2. XRD measurements confirm that the functionalization of vanadium oxide layers with longer amine molecule chains increases the resulting VONT periodic spacing as expected if a similar intercalation and stacking mechanism holds, as found for dodecyl- and hexadecylamine. The effect of molar ratio variation on periodic spacing does not appear as significant in bulk powder quantities, as shown from TEM measurements of the periodic spacing of many individual VONTS in Fig. 6(b). XRD measurements also include contributions to (00*l*) reflections layer spacing for unreacted xerogel material. Thus, Fig. 6(a) suggests that any (re)precipitated vanadium oxide materials devoid of amines, or indeed remnant material that was in excess, does not crystallize to a layered, hydrated V_2O_5 structure that contributes to the Bragg reflections in XRD. Using the approach described in Fig. 2(e), we carefully measured the periodic spacing for all VONTs synthesized in the series comprising 21 sets of syntheses, *i.e.* for each

xerogel:amine ratio, for each length of amine used. The amine molecular lengths used were 0.9758 nm (hexylamine), 1.7435 nm (dodecylamine) and 2.5112 nm (octadecylamine). The periodic spacing refers to the V_2O_5 lamina thickness in the VONT in addition to the interlayer spacing occupied by the amine bilayer between two lamina. This overall value is also the spacing associated with the (001) periodicity determined by XRD. Figure 6(b) shows the comparative measured periodic spacing determined by analysis of many individual VONTs by HRTEM. It is clear that the periodic spacing increases with amines of longer nominally unfolded and defect-less molecular length. A linear relationship was observed between the periodic spacing and length of amine molecule for the majority of molar ratios of xerogel:amine that were investigated. The exceptions were VONTs prepared with amines in excess of the vanadium oxide (xerogel:amine of 1:4, 1:3).

The measured periodic spacings, determined using TEM of a random selection of VONTs prepared with excess octadecylamine are significantly larger than for VONTs prepared with excess hexylamine and dodecylamine (see Fig. 7). This may be the result of an increased packing density of longer amine molecules. Previous examination of thiols within vanadium oxides, and amines within layered nanoscale clays, have shown that changes in the conformation of certain amines can also affect interlayer spacings for a given packing density [54, 55, 62, 66]. In such cases, extended chains in the bilayer or a lesser degree of interdigitation can alter the spacing width. The exact mechanism however, is not entirely clear and the subject of significant debate in hybrid and lamellar materials synthesis.

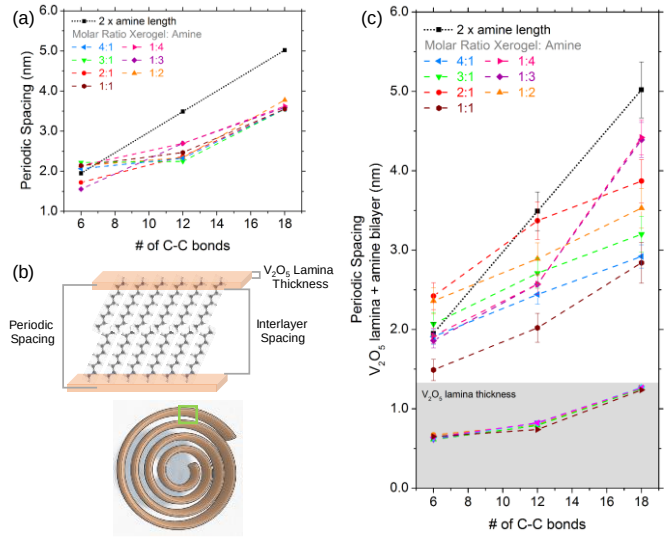

Fig. 6. (a) Interlayer spacing measurements caused by intercalated amine molecules between V_2O_5 layers in VONTs determined from (a) XRD analysis of bulk powder quantities and (b) (*Top*) HRTEM measurements of a random selection of VONTs and (*Bottom*) HRTEM measurements of the width of the V_2O_5 lamina within VONTs for the entire series of syntheses using hexylamine, dodecylamine and octadecylamine. (c) Schematic representation of the V_2O_5 lamina spacing, the periodic spacing and the interlayer spacing of a scrolled VONT.

As the water content of the V_2O_5 lamina can affect thickness and thus the periodic spacing, we also measured a range of lamina thickness by HRTEM and compared them to the overall periodic spacing in Fig. 6(b). Crystal water is assumed to be accounted for in the measured V_2O_5 thickness post-synthesis and any additional water within the spacing occupied by the amines may affect the measurements. Figure 6(b) shows that the lamina thickness increases as a result of synthesis with longer amines, but with a similar synthetic content of water. The periodic spacing, as mentioned above, and shown in Fig. 6(b), increases linearly with the number of C-C bonds. Thus, the difference in the two sets of measurements gives the specific interlayer spacing in which the amines reside. Figure 6(b) confirms that both the periodic spacing and the interlayer spacing are dominantly controlled by the intercalating bilayer of amines, and that the nature of the packing is self-similar through the ranges of amine lengths from n = 6 – 18. If we assume that all well-packed amine bilayers are hydrophobic as has been well-established, and that additional water molecules that may be present within the layer do not add a van der Waals diameter of ~0.28 nm (per molecule) to the values of the periodic spacing, then the increasing V_2O_5 lamina thickness is postulated to be due to less efficient intercalation of the 2D layered structures by the much larger amines, i.e. the V_2O_5 thickness with ordered octadecylamine molecules is twice that when hexylamines are intercalated, even though the periodic spacing is relatively consistent.

The resulting sheet thickness is defined by the length of the amine used and is reasonably independent of molar ratio. The interlayer spacing is defined by the interdigitation of the amine bilayer template and the packing density of the amine molecules within the layers. Shorter molecules tend to intercalate into V_2O_5 in a manner that maximizes the number of interlayer spacings; previous investigation corroborate these findings for various different intercalated organics and the thickness of the V_2O_5 walls can comprise up to 10 molecular sheets in some cases [36, 49, 69-73].

As the theoretical thickness of a single crystal V_2O_5 bilayer present in bulk crystalline V_2O_5 is ~0.5 nm, the data shows that effectively two bilayers of vanadium oxide, as a crystalline slab are intercalated with longer molecules, while single bilayers are intercalated with shorter molecules. This trend shows that the size of the organic template can influence the number of layers found in VONTs, but also could be a factor in the many layered hybrid organic-inorganic materials where organic templates are intercalated into van der Waals gallery spacings that prop apart inorganic crystalline sheets.

All of the VONTs synthesized with dodecylamine and octadecylamine as well as the majority of the VONTs synthesised with hexylamine exhibited interlayer spacings < $2l_{mol}$. This confirms an interdigitation of a bilayer of amines on juxtaposed V_2O_5 surface within each gallery spacing. Interdigitation has been observed in related systems using amines and thiols [62, 74]. Figure 6(b) demonstrates that a controlled interlayer spacing can be obtained by the incorporation of amine molecules of different lengths, for n > 6. The VONT interlayer spacing is dependent not only on the length of the amine molecule and how they interact but also on the density of organic molecules on the surface of the

inorganic phase and how the overall packing density maintains interlayer spacing throughout the layer [62]. Once intercalated, the data shows that the packing density and thus the spacing is directly affected by the choice of xerogel:amine ratio. The vanadium oxide interlayer spacings likely feature electrostatically bound amine chains with additional amine molecules interspersed but not chemically bound to the V_2O_5 substrate. In this work it is assumed that the amine binding sites are identical in all cases and the packing density of the amines is only varied by differences in amine quantity and molecular length. To reaffirm that analysis of these measurements, a series of histograms detailing the variation in >100 individual measurements from TEM images of VONT samples shown in Fig. 4, are provided in Fig. 7. Correlation of interlayer spacing measurements for both TEM and XRD confirm that longer amine molecules result in wider interlayer spacings – interdigitation that reduced the spacing to $<2l_{mol}$ is not found to be affected by molecule length, but packing density.

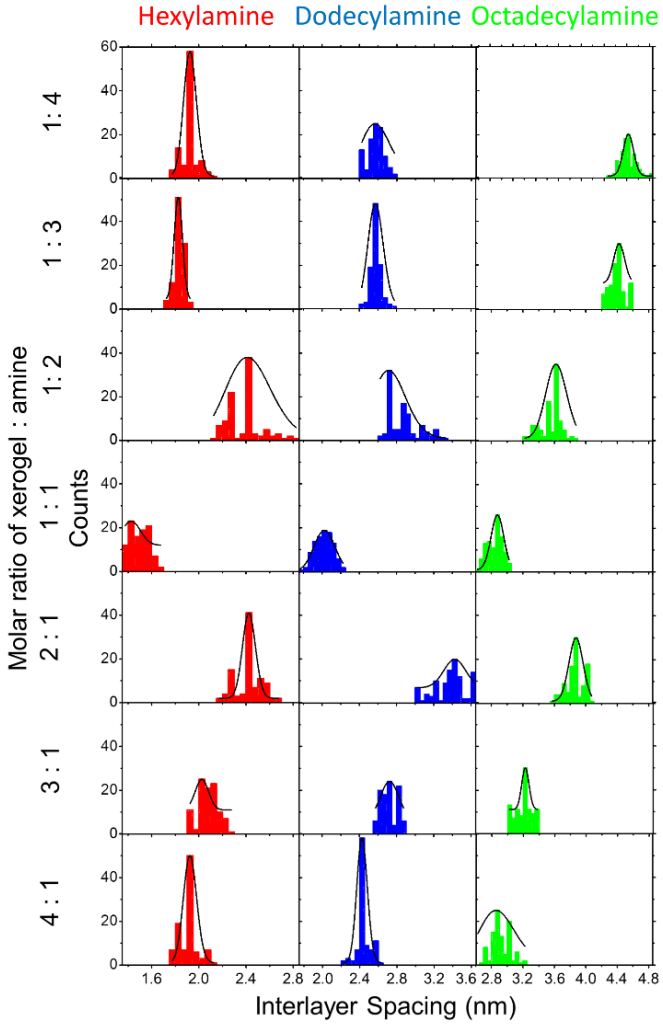

Fig. 7. Frequency of interlayer spacings measured from 100 individual measurements from HRTEM images of VONTs synthesised using hexylamine, dodecylamine and octadecylamine molecules in each of the xerogel:amine ratios.

Vibrational spectroscopy of VONT organic-inorganic structure

The quality, consistency and details of the structure of VONTs is best probed by considering both the inorganic and organic constituents, how they interact to form and maintain a consistent scroll, and the specific differences in the final structure from each synthesis. In order to compare the synthesized inorganic-organic nanotubes at the molecular-interaction level, FTIR spectra were acquired from VONTs synthesized using hexylamine, dodecylamine and octadecylamine for all synthetic ratios (from 1:4 to 4:1) and are presented in Fig. 8. Some features are common to all of the spectra that were acquired. The absorption that occurs at between 720 – 730 cm^{-1} is attributed to lattice vibration of V_2O_5. [51, 75] The peaks observed between 2850-2930 cm^{-1} and 1460-1650 cm^{-1} are due to C-H stretching and bending vibrations respectively. [51, 66, 76, 77] The intensity of these peaks increases with the amine chain length due to the presence of a greater number of C-H bonds within the vanadium oxide layers. Evidence can also be seen in FTIR spectra to support the growth mechanism for VONTs discussed earlier. The V=O bond present in bulk V_2O_5 powder gives an absorption peak at around 1040 cm^{-1}, as outlined in the IR analysis of the synthesis steps in Fig. S3, Supplementary Information. The intensity of the peak observed at this value for VONT materials is greatly reduced. This suggests that the reduction of the V=O bond by hydroxide ions, as discussed earlier, likely occurs. The broad band beginning at 3040 cm^{-1} is assigned to ammonium ions implying that the NH_2 head group of the amine molecules are present in the vanadium oxide layers as NH_3^+. Another broad band beginning at 3300 cm^{-1} is attributed to the stretching and bending modes of O-H vibrations [78, 79].

The frequencies are distinctly different to those of crystal water, which is removed during several days of HT. The lack of an appreciable broadband bump from O-H vibrations confirms a nominally hydrophobic environment within the packed amine bilayer, even with xerogel in excess, confirming hydration of both intercalation and unreacted, crystallized V_2O_5. The presence of vibrations attributed to NH^{3+} groups, and the low relative intensity of vibrations associated with V=O bonds all support the VONT growth mechanism discussed above.

The FTIR spectra in Fig. 8 (a) show a greater measured response from $V–O^-$ vibrations than from V=O for VONTs prepared with hexylamine. However, the intensity of V=O vibrations is greater than the intensity of $V–O^-$ vibrations for VONTs prepared with longer amines at 1:2, 2:1, 1:3 and 3:1 mixture ratios (Fig. 8 (b) and (c)). For excess amines, the reduced vanadyl bond vibration band widens, indicating a greater quantity of interaction with electrostatically bound amines as the VONT forms and scrolling deformation of the lattice takes place in tandem. The data also confirm that hexylamine VONTs are of high quality, in agreement with TEM examination of the tubular structure, and the consistency in structure (specifically the broader band of $V\text{-}O^-$ vibration commensurate with reduction via electrolysis of amines that subsequently functionalize the V_2O_5 surfaces) throughout the full range of xerogel:amine mixtures ratios is found. As

previously mentioned, the peaks located in the range of 2700-3000 cm^{-1}, are associated with symmetric and asymmetric CH_2 and CH_3 modes – all 4 stretching modes are observable in VONTs from all syntheses. Importantly, the modal frequencies are consistent with those observed for similar length primary thiols (62) intercalated in V_2O_5, and confirm that high quality ordering of amines occurs in the low yield of preferentially formed VONTs when synthesized with limited amines (xerogel in excess). The intensity of these peaks is found to be lowest for shorter chained amines.

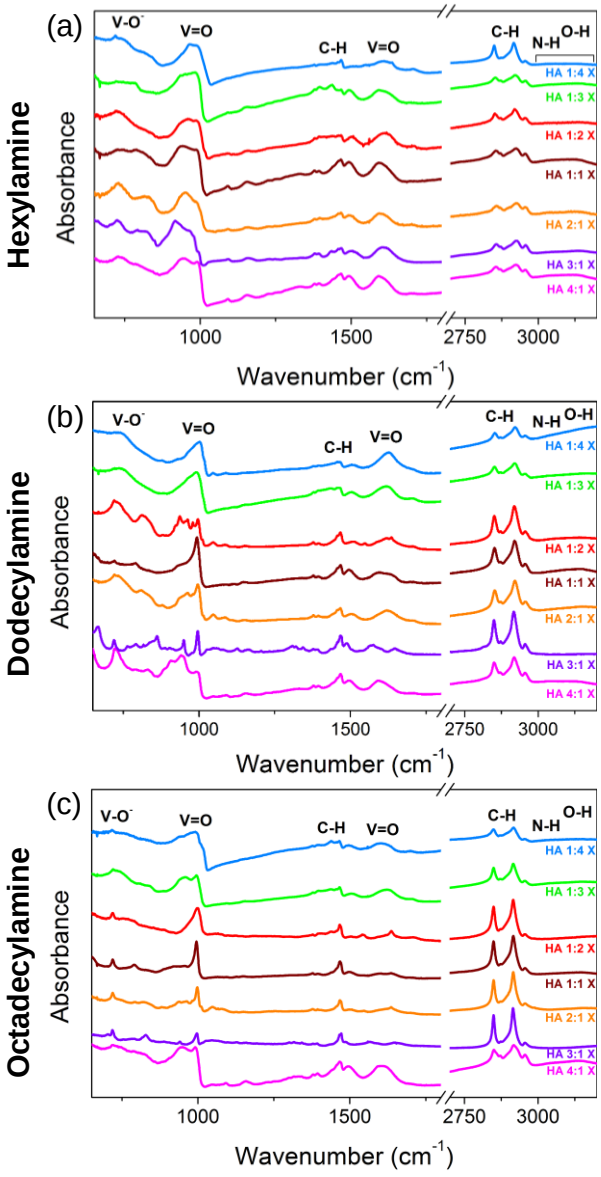

Fig. 8. FTIR spectra for all xerogel: amine mixture ratios for VONTs synthesized using (a) hexylamine, (b) dodecylamine and (c) octadecylamine.

In order to observe the importance of the amines in VONT formation, quality and yield during synthesis, a hydrothermal treatment of the xerogel under the same conditions without amine addition was performed and the resulting product is shown in Fig. 9(a). Without intercalated amines, the scrolling is neither initiated nor maintained and consequently VONTs were not formed. A mixture of xerogel and dodecylamine (molar ratio 1:2, respectively) was thermally treated without the addition of water to determine the effect of water on VONT formation under identical conditions. The product of this reaction is shown in Fig. 9(b). Without added water prior to HT, VONTs were not formed. The V_2O_5, being easily reduced, requires the presence of water to hydrolyze the amino group and facilitate electrostatic binding with the reduced $V\text{-}O^-$ species at the surface. The dedicated measurements of VONT quality during synthesis under identical, controlled conditions, and the necessity for water and amines reaffirms some aspects of the debate surrounding curvature formation and consistent interlayer spacing. Previous theories have reported that the hydroxyl groups in 2-propanol (like ethanol, added as the reductant) are oxidized to ketones by the V^{5+}; the smaller the 2-propanol content, the smaller the V^{4+}/V^{5+} ratio. Our measurement shows that without water in the ethanolic mixture, scrolling facilitated in part for V^{5+} reduction, does not occur without added water.

Amines must be either in a 2:1 ratio with V_2O_5 or in excess, and water must hydrolyze them, while the V_2O_5 accommodate a bilayer of amines between the vdW spacings via intercalation. With larger V^{4+} ionic radius, which is presumed to contribute to curvature formation since its size must be accommodated (ionic radius of V^{4+} is approx. twice that of V^{5+}), a constant distance is maintained between layers in a VONT only if amines are present, which is facilitated by electrostatic interactions at their preferred packing density for a given length when V^{4+} is present, and thus a balance of forces is postulated to maintain the VONT scrolling, as proven in nanofibers with intercalated thiol species. Here however, the reduction process causes scrolling to accommodate larger ions and the consistency in the radius or curvature depends on a uniform 2D spatial distribution of V^{4+} sites to prevent twisting or other defects (e.g. gauche) [80] in the unidirectional scrolling vector of the lamina. From a synthetic yield perspective, the quality of the VONTs requires ideal packing density of amines for a given length to maintain a perfect scroll, but also a uniform degree of amine binding events across the V_2O_5 interlayers surfaces. Less effective coverage of the V_2O_5 layers reduces the number and areal density of lattice sites (V^{4+}/V^{5+} distribution) on the V_2O_5 the reduction upon amine intercalation. Such a reduction in larger V^{4+} ionic sites locally reduces the degree of bending that accommodates those volume changes within the lattice, affecting the smoothness of the scroll in places.

The excess amines in the experiments promote maximal interlayer packing of amines by ensuring sufficiently high local concentrations of molecules for intercalation between the substrate layers, with some of the remainder forming an amine 'sheath' surrounding the VONTs, as shown in Fig. 9 (c). This observation is quite common for syntheses involving 1:3 and 1:4 xerogel:amine ratios. The diffusion of amines out of the interlayer region is unlikely since they are in excess and changes in the Hildebrand solubility parameter under hydrothermal conditions (reduced dielectric constant and

increased water ionization constant) in mixed solvents such as EtOH/H_2O does not promote outflux of already intercalated amines.

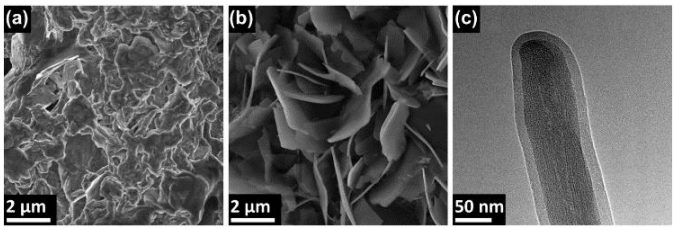

Fig. 9. SEM images of products after thermal treatment (a) without amines (b) without water. (c) TEM image of organic layer surrounding VONTs synthesized with excess amines.

Comparison with vanadium oxide nanofibers (again composed of layered V_2O_5 sheets) in which organic molecules (primary thiols) can be intercalated [62, 66], has shown that at high packing densities of 9.8 chains nm^{-2}, the interlayer spacing of ~2.5 nm (similar to the measured value of 2.4 nm in VONTs, but using dodecanethiol), gave unstable dynamics corresponding to a cramped, unrealistic intercalated bilayer. However, a wider 3.0 nm spacing, gave stable dynamics for this simulation. In the context of the present results, it confirms that excess amines can, through enough measurements with statistical significance, widen the layer spacing beyond $2l_{mol}$.

Multiscale chain defects that affect VONT formation: Non-uniformities in amine packing and V_2O_5 lamina scrolling

Occasionally when the products of these syntheses were imaged by TEM certain non-uniformities in the as-synthesized VONTs were observed, as shown in Fig. 10. These non-uniformities can be divided into four different groups. (i) A bending or buckling of the intercalated V_2O_5 layers: These bends are most likely a result of differences in the packing density of amine molecules along the length of the juxtaposed V_2O_5 basal surfaces in each periodic spacing [66]. In this scenario, it is presumed that the interdigitated amines maintain a consistent interlayer spacing and that energy derived from HT conditions allow buckling of the crystalline V_2O_5 lamina, but these bends and buckles almost uniquely occur when the interlayer spacing reduces, i.e. there is a collapse of intercalated amines or there are pockets or vdW space where laminar compression can occur more easily. (ii) A non-hollow core: The characteristic core of the proper VONTs is hollow throughout, but partial tube blocking is sometimes observed. A possible collapse of the layered walls in the centre of the nanotube may result in the appearance of a filled core. (iii) Spiraling: VONTs that demonstrate the spiraling non-uniformity are caused by the diagonal scrolling of an amine intercalated layered sheet of V_2O_5. The apparent chirality and characteristic spiral angle are related to the corner-first initiation of scrolling of a rectangular lamina (see schematic and Fig. 10). Due to spiraling, consistent parallel flanking V_2O_5 lamina are not observed in TEM images. (iv) Twisting: The twisting non-uniformity may be the result of scrolling mechanisms competing in different directions within the same layered V_2O_5 structure. From analysis of multiple VONTs from each syntheses, we find that these groups constitute the primary non-uniformities in VONTs, and they are more common (although with low frequency compared to 'standard' VONTs at high xerogel:amine ratios (excess xerogel).

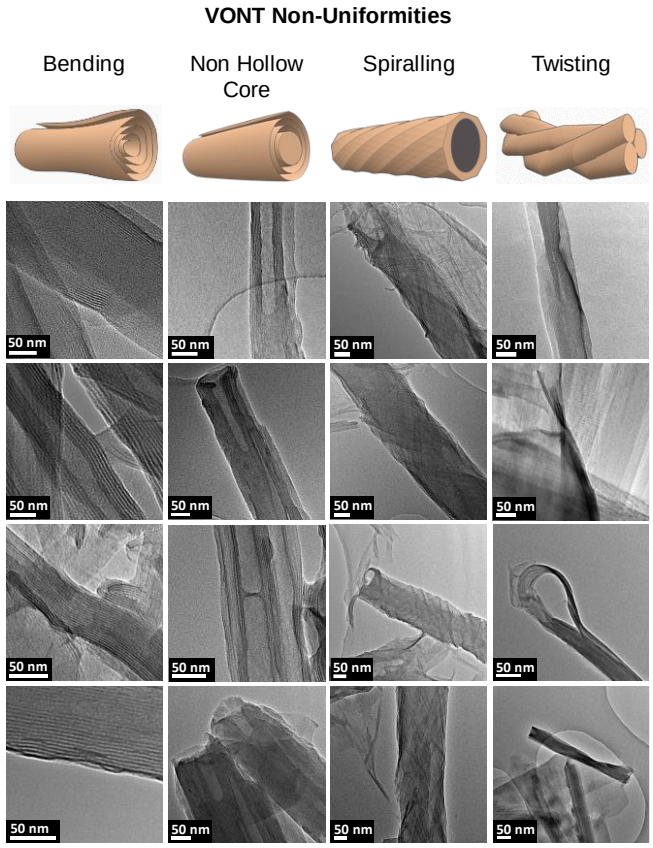

Fig. 10. TEM images of the 4 categories of non-uniformities observed in VONTs grown by hydrothermal treatment using V_2O_5 xerogel and primary alkylamines.

Conclusions

The systematic investigation of the synthetic conditions that influence the structure, morphological uniformity and yields of vanadium oxide nanotubes has been investigated. Using a range of amine templates ranging from short hexylamine to the longer didecylamine, high resolution spectroscopies and microscopies have identified the dependence on amine length and xerogel:amine mixture ratios that influence the VONT structure.

The quality of VONTs is optimized by V_2O_5 xerogel and amine mixture ratio. Excess amines can result in expansion of the interlayer spacing and a reduction in the statistical consistency in the inlayer spacing value. Using a nominal V_2O_5:amine ratio of 1:2, maximizes coverage of amine attachment sites to juxtaposed V_2O_5 layers within the VONTs and results in consistent interlayer spacings throughout the synthetic product. The consistency in structure, as determined using FTIR, electron microscopy and XRD, is improved when shorter chained amines are used. This is also the first time

several primary amines have been successfully applied to VONT synthesis and the consistency in uniformity for a range of xerogel:amine mixture ratios is due to the reduced thickness of the vanadium oxide sheets comprising the structure and strong van der Walls forces resulting a narrower interlayer spacing. The analysis of crystallographic and periodic diffraction contributions suggests that the additional peaks in the diffraction patterns result from variation in interlayer spacings or so-called 'interstratified' structures.

The thickness of the V_2O_5 sheets is found for the first time to be correlated on the length of the organic (amine) molecule, which itself dictates that nature of the hydrophobic interlayer environment. For amine lengths < 9 C-C bonds, the V_2O_5 sheet thickness approaches that of a single V_2O_5 crystalline bilayer. Although difficult to experimentally control in hydrothermal syntheses, this result implies that for a given thickness of starting xerogel, and sufficient concentration of ~2 amines per V_2O_5 unit, the number of periodic layer spacings is greater when using shorter chain length intercalative organic templates. XRD analysis confirms that the use of longer amine chains results in wider VONT interlayer spacings. High angle reflections remain relatively consistent when both amine length and molar ratios are varied.

A range of non-uniformities in VONT samples were observed, including bending, spiraling, twisting and a non-hollow core. The frequency of these defects in the products of the hydrothermal reaction is not very high. However, their presence indicates the ability of the organic-inorganic layered structure to accommodate curvature without delamination or cleaving.

From the standard syntheses that facilitate high mass product yield of VONTs and indeed other vanadium oxide based nanomaterials, the correlation between synthesis conditions and both yield and uniformity or quality of the materials has important implications for their applications. Layered compounds are often exploited for the properties of their layered structure, and in high yield requirements, control of this parameter is critical. In electrochemical applications, particularly in Li-ion and related batteries, the interlayer spacing is important for fast and efficient ion intercalation and reaction, and for redox pseudocapacitance. In electrodes with high mass loading, the uniformity and consistency in layer spacing affects the intercalation rate and specific capacity, and helps to minimize volumetric expansion effects that limit cycle life.

Methods

Synthesis of Vanadium Oxide Nanotubes

A series of vanadium oxide nanotubes (VONTs) were synthesized by mixing of a lamellar-structured V_2O_5 xerogel precursor with a range of long-chain primary amines acting as structure-maintaining templates under hydrothermal treatment (HT). Initially, 1 g of bulk V_2O_5 powder (Sigma Aldrich) was mixed with 90 ml of *tert*-butanol and heated under reflux at 100 °C. The yellow solution obtained after vigorous stirring for 6 hours was then hydrolyzed by adding 30 ml of deionized water. Adding the water changed the colour of the solution from yellow to orange. The solvent was then evaporated to form a dried vanadium oxide xerogel. This xerogel was mixed with primary amines in a series of molar ratios of xerogel: amine ranging from 1:4 to 4:1 inclusively. The amines used were primary amines ranging from hexylamine (6 C-C) to ocatadecylamine (18 C-C). A didecylamine (10 C-C chains bound either side of the terminal N-H group) was also used to alter the binding condition with V_2O_5 to examine the dependence on head groups reduction and electrostatic binding. An example of a preparation mixture, for xerogel mixed with hexylamine (HA) in a molar ratio of xerogel: amine of 2:1 is as follows: 0.3 g xerogel was mixed with 0.083 g of HA and 3 ml of ethanol was added per gram of xerogel. The solution was mixed vigorously for 1 h and then hydrolyzed by adding 5 ml of deionized water per gram of xerogel before being mixed vigorously again for a further two hours. The mixture was then allowed to age for 2 days, during which time the mixture turned white. It was then hydrothermally treated in a Teflon lined autoclave at 180 °C for 7 days. The resulting dark paste was filtered through Whatman grade 1 filter paper, washed with pure ethanol and dried using a Büchner funnel. Drying in this manner for approximately 4 hours produced a dry black powder consisting of VONTs.

Methods of Characterization

TEM analysis was conducted using a field emission JEOL JEM-2100F microscope operating at an accelerating voltage of 200 kV. Interlayer distance measurements were taken from high resolution TEM data. SEM analysis was performed using a Hitachi S-4800 at an accelerating voltage of 10 kV. XRD analysis was performed using an X'pert MRDpro Panalytical instrument using Cu Kα radiation. (Cu Kα, λ = 0.15418 nm, operation voltage 40 kV, current 30 mA). FTIR spectra were recorded using a Perkin-Elmer Spectrum 100 spectrometer in the range 650 – 4000 cm^{-1}.

Acknowledgements

This publication has emanated from research conducted with the financial support of the Charles Parsons Initiative and Science Foundation Ireland (SFI) under Grant No. 06/CP/E007. Part of this work was conducted under the framework of the INSPIRE programme, funded by the Irish Government's Programme for Research in Third Level Institutions, Cycle 4, National Development Plan 2007-2013. This work was also supported by an SFI Technology Innovation and Development Award under contract no. 13/TIDA/E2761. This research has received funding from the Seventh Framework Programme FP7/2007-2013 (Project STABLE) under grant agreement no. 314508. We also acknowledge the support of the Irish Research Council under a New Foundations Award. This publication has also emanated from research supported in part by a research grant from SFI under Grant Number 14/IA/2581.

References

1. C. N. R. Rao and M. Nath, *Dalton Trans.*, 2003, **0**, 1-24.
2. R. H. Baughman, A. A. Zakhidov and W. A. de Heer, *Science*, 2002, **297**, 787-792.
3. S. Ryu, P. Lee, J. B. Chou, R. Xu, R. Zhao, A. J. Hart and S.-G. Kim, *ACS Nano*, 2015, **9**, 5929-5936.
4. C. K. Chan, H. Peng, G. Liu, K. McIlwrath, X. F. Zhang, R. A. Huggins and Y. Cui, *Nat. Nanotechnol.*, 2008, **3**, 31-35.
5. W. Zhou, X. Dai, T.-M. Fu, C. Xie, J. Liu and C. M. Lieber, *Nano Lett.*, 2014, **14**, 1614–1619.
6. W. C. Lee, K. Kim, J. Park, J. Koo, H. Y. Jeong, H. Lee, D. A. Weitz, A. Zettl and S. Takeuchi, *Nat. Nanotechnol.*, 2015, **10**, 423-428.
7. P. G. Bruce, B. Scrosati and J.-M. Tarascon, *Angew. Chem. Int. Ed.*, 2008, **47**, 2930-2946.
8. W. Lu and C. M. Lieber, *Nat. Mater.*, 2007, **6**, 841-850.
9. L. Xu, Z. Dai, G. Duan, L. Guo, Y. Wang, H. Zhou, Y. Liu, W. Cai, Y. Wang and T. Li, *Sci. Rep.*, 2015, **5**, 10507.
10. A. J. Gellman and N. Shukla, *Nat. Mater.*, 2009, **8**, 87-88.
11. F. Cheng, Z. Tao, J. Liang and J. Chen, *Chem. Mater.*, 2007, **20**, 667-681.
12. Y. Wang and G. Cao, *Chem. Mater.*, 2006, **18**, 2787-2804.
13. C. N. R. Rao, B. C. Satishkumar, A. Govindaraj and M. Nath, *ChemPhysChem*, 2001, **2**, 78-105.
14. J. Macak, H. Tsuchiya, A. Ghicov, K. Yasuda, R. Hahn, S. Bauer and P. Schmuki, *Curr. Opin. Solid State Mater. Sci.*, 2007, **11**, 3-18.
15. P. Ramasamy, D.-H. Lim, J. Kim and J. Kim, *RSC Adv.*, 2014, **4**, 2858-2864.
16. Z. Chen, Y. Qin, D. Weng, Q. Xiao, Y. Peng, X. Wang, H. Li, F. Wei and Y. Lu, *Adv. Funct. Mater.*, 2009, **19**, 3420-3426.
17. R. Ostermann, D. Li, Y. Yin, J. T. McCann and Y. Xia, *Nano Lett.*, 2006, **6**, 1297-1302.
18. X. Xie, Y. Li, Z.-Q. Liu, M. Haruta and W. Shen, *Nature*, 2009, **458**, 746-749.
19. J. Lu, Q. Peng, W. Wang, C. Nan, L. Li and Y. Li, *J. Am. Chem. Soc.*, 2013, **135**, 1649-1652.
20. M. S. Whittingham, *J. Electrochem. Soc.*, 1976, **123**, 315-320.
21. D. McNulty, D. N. Buckley and C. O'Dwyer, *J. Power Sources*, 2014, **267**, 831-873.
22. J. Schoiswohl, S. Surnev, F. Netzer and G. Kresse, *J. Phys.: Condens. Matter*, 2006, **18**, R1.
23. W. Avansi Jr, C. Ribeiro, E. R. Leite and V. R. Mastelaro, *Cryst. Growth Des.*, 2009, **9**, 3626-3631.
24. G. Li, K. Chao, H. Peng, K. Chen and Z. Zhang, *Inorg. Chem.*, 2007, **46**, 5787-5790.
25. C. Wu and Y. Xie, *Energy Environ. Sci.*, 2010, **3**, 1191-1206.
26. J. Livage, *Chem. Mater.*, 1991, **3**, 578-593.
27. Y. Wang, K. Takahashi, K. H. Lee and G. Cao, *Adv. Funct. Mater.*, 2006, **16**, 1133-1144.
28. N. A. Chernova, M. Roppolo, A. C. Dillon and M. S. Whittingham, *J. Mater. Chem.*, 2009, **19**, 2526-2552.
29. N. Steunou and J. Livage, *CrystEngComm*, 2015, **17**, 6780-6795.
30. J. Livage, *Coord. Chem. Rev.*, 1998, **178**, 999-1018.
31. M. Sathiya, A. Prakash, K. Ramesha, J. M. Tarascon and A. Shukla, *J. Am. Chem. Soc.*, 2011, **133**, 16291-16299.
32. D. McNulty, D. N. Buckley and C. O'Dwyer, *J. Electrochem. Soc.*, 2014, **161**, A1321-A1329.
33. C. O'Dwyer, V. Lavayen, D. A. Tanner, S. B. Newcomb, E. Benavente, G. Gonzalez and C. M. S. Torres, *Adv. Funct. Mater.*, 2009, **19**, 1736-1745.
34. D. Su and G. Wang, *ACS Nano*, 2013, **7**, 11218-11226.
35. H.-Y. Li, C.-H. Yang, C.-M. Tseng, S.-W. Lee, C.-C. Yang, T.-Y. Wu and J.-K. Chang, *J. Power Sources*, 2015, **285**, 418-424.
36. M. E. Spahr, P. Bitterli, R. Nesper, M. Müller, F. Krumeich and H. U. Nissen, *Angew. Chem. Int. Ed.*, 1998, **37**, 1263-1265.
37. S. Iijima, *Nature*, 1991, **354**, 56-58.
38. G. Radovsky, R. Popovitz-Biro and R. Tenne, *Chem. Mater.*, 2012, **24**, 3004-3015.
39. P. J. Hagrman, D. Hagrman and J. Zubieta, *Angew. Chem. Int. Ed.*, 1999, **38**, 2638-2684.
40. S. Inagaki, S. Guan, Y. Fukushima, T. Ohsuna and O. Terasaki, *J. Am. Chem. Soc.*, 1999, **121**, 9611-9614.
41. Q. Wang and D. O'Hare, *Chem. Rev.*, 2012, **112**, 4124-4155.
42. Q. Wang, X. Zhang, J. Zhu, Z. Guo and D. O'Hare, *Chem. Commun.*, 2012, **48**, 7450-7452.
43. Q. H. Wang, K. Kalantar-Zadeh, A. Kis, J. N. Coleman and M. S. Strano, *Nat. Nanotechnol.*, 2012, **7**, 699-712.
44. A. Ayari, E. Cobas, O. Ogundadegbe and M. S. Fuhrer, *J. Appl. Phys.*, 2007, **101**, 014507.
45. S. Kobayashi, N. Hamasaki, M. Suzuki, M. Kimura, H. Shirai and K. Hanabusa, *J. Am. Chem. Soc.*, 2002, **124**, 6550-6551.
46. K. J. van Bommel, A. Friggeri and S. Shinkai, *Angew. Chem. Int. Ed.*, 2003, **42**, 980-999.
47. J. Zhu, L. Cao, Y. Wu, Y. Gong, Z. Liu, H. E. Hoster, Y. Zhang, S. Zhang, S. Yang, Q. Yan, P. M. Ajayan and R. Vajtai, *Nano Lett.*, 2013, **13**, 5408-5413.
48. A. Pan, H. B. Wu, L. Yu, T. Zhu and X. W. Lou, *ACS Appl. Mater. Interfaces*, 2012, **4**, 3874-3879.
49. M. Niederberger, H.-J. Muhr, F. Krumeich, F. Bieri, D. Günther and R. Nesper, *Chem. Mater.*, 2000, **12**, 1995-2000.
50. G. T. Chandrappa, N. Steunou, S. Cassaignon, C. Bauvais and J. Livage, *Catal. Today*, 2003, **78**, 85-89.
51. W. Chen, J. Peng, L. Mai, Q. Zhu and Q. Xu, *Mater. Lett.*, 2004, **58**, 2275-2278.
52. X. Chen, X. Sun and Y. Li, *Inorg. Chem.*, 2002, **41**, 4524-4530.
53. V. Lavayen, C. O'Dwyer, G. Cárdenas, G. González and C. Sotomayor Torres, *Mater. Res. Bull.*, 2007, **42**, 674-685.
54. G. Lagaly, *Solid State Ion.*, 1986, **22**, 43-51.
55. H. J. M. Hanley, C. D. Muzny, D. L. Ho and C. J. Glinka, *Langmuir*, 2003, **19**, 5575-5580.

56. J.-J. Lin and Y.-M. Chen, *Langmuir*, 2004, **20**, 4261-4264.
57. D. McNulty, D. N. Buckley and C. O'Dwyer, *ECS Trans.*, 2011, **35**, 237-245.
58. V. Petkov, P. Zavalij, S. Lutta, M. Whittingham, V. Parvanov and S. Shastri, *Phys. Rev., B*, 2004, **69**, 085410.
59. L. I. Vera-Robles and A. Campero, *J. Phys. Chem. C*, 2008, **112**, 19930-19933.
60. M. Jaber, F. o. Ribot, L. Binet, V. r. Briois, S. Cassaignon, K. Rao, J. Livage and N. Steunou, *J. Phys. Chem. C*, 2012, **116**, 25126-25136.
61. T. Rostamzadeh, S. Adireddy, X. Zhang, B. Koplitz, D. B. Chrisey and J. B. Wiley, *ChemNanoMat*, 2016, **2**, 54-60.
62. G. Gannon, C. O'Dwyer, J. A. Larsson and D. Thompson, *J. Phys. Chem. B*, 2011, **115**, 14518-14525.
63. F. Krumeich, H.-J. Muhr, M. Niederberger, F. Bieri, M. Reinoso and R. Nesper, *Mater. Res. Soc. Symp. Proc.*, 1999, **581**.
64. G. T. Chandrappa, N. Steunou, S. Cassaignon, C. Bauvais, P. K. Biswas and J. Livage, *J. Sol-Gel Sci. Technol.*, 2003, **26**, 593-596.
65. G. Ferey, *Dalton Trans.*, 2016, DOI: 10.1039/C5DT03547C.
66. C. O'Dwyer, G. Gannon, D. McNulty, D. N. Buckley and D. Thompson, *Chem. Mater.*, 2012, **24**, 3981-3992.
67. B. Casal, E. Ruiz-Hitzky, M. Crespin, D. Tinet and J. Galvan, *J. Chem. Soc., Faraday Trans.*, 1989, **85**, 4167-4177.
68. O. Durupthy, N. Steunou, T. Coradin and J. Livage, *J. Phys. Chem. Solids*, 2006, **67**, 944-949.
69. F. Krumeich, H. J. Muhr, M. Niederberger, F. Bieri, B. Schnyder and R. Nesper, *J. Am. Chem. Soc.*, 1999, **121**, 8324-8331.
70. G. R. Patzke, F. Krumeich and R. Nesper, *Angew. Chem. Int. Ed.*, 2002, **41**, 2446-2461.
71. H. J. Muhr, F. Krumeich, U. P. Schönholzer, F. Bieri, M. Niederberger, L. J. Gauckler and R. Nesper, *Adv. Mater.*, 2000, **12**, 231-234.
72. F. Bieri, F. Krumeich, H.-J. Muhr and R. Nesper, *Helv. Chim. Acta.*, 2001, **84**, 3015-3022.
73. K. S. Pillai, F. Krumeich, H.-J. Muhr, M. Niederberger and R. Nesper, *Solid State Ion.*, 2001, **141**, 185-190.
74. C. O'Dwyer, V. Lavayen, D. Fuenzalida, H. Lozano, M. A. Santa Ana, E. Benavente, G. Gonzalez and C. M. S. Torres, *Small*, 2008, **4**, 990-1000.
75. B. Azambre, M. Hudson and O. Heintz, *J. Mater. Chem.*, 2003, **13**, 385-393.
76. J. Liu, X. Wang, Q. Peng and Y. Li, *Adv. Mater.*, 2005, **17**, 764-767.
77. F. Sediri, F. Touati and N. Gharbi, *Mater. Lett.*, 2007, **61**, 1946-1950.
78. E. Sabbar, M. De Roy and J. Besse, *J. Solid State Chem.*, 2000, **149**, 443-448.
79. L. Vera-Robles, F. Naab, A. Campero, J. Duggan and F. McDaniel, *Nucl. Instr. Meth. Phys. Res.*, 2007, **261**, 534-537.
80. A. Kiersnowski, K. Kolman, I. Lieberwirth, S. Yordanov, H.-J. Butt, M. R. Hansen and S. H. Anastasiadis, *Soft Matter*, 2013, **9**, 2291-2301.